Insight into effects of high intensity ultrasound treatment on foamability and physicochemical properties of frozen egg white protein

Ya Li
Nanjing University of Finance and Economics/Collaborative Innovation Center for Modern Grain Circulation and Safety

Ling Yu
Nanjing University of Finance and Economics/Collaborative Innovation Center for Modern Grain Circulation and Safety

Lifeng Wang
Nanjing University of Finance and Economics/Collaborative Innovation Center for Modern Grain Circulation and Safety

Wenfei Xiong (wenfeixiong@nufe.edu.cn)
Nanjing University of Finance and Economics/Collaborative Innovation Center for Modern Grain Circulation and Safety

Research Article

Keywords: High intensity ultrasound, Egg white protein, Foaming, Interfacial adsorption

Posted Date: August 18th, 2022

DOI: https://doi.org/10.21203/rs.3.rs-1959549/v1

Abstract

Frozen storage can greatly improve the shelf life of fresh egg white protein (EWP), but at the same time, it will also lead to the reduction of protein foaming and can not meet the application needs. Herein, high-intensity ultrasound (HIUS) was used to improve the foam characteristics of EWP in different frozen storage periods. The results showed that compared with fresh egg white, the foaming ability of EWP with different freezing times (0, 3, 7, 14, 21 days) after HIUS treatment (20 kHz, 60% amplitude, 5 min) was significantly improved, especially the EWP after 21 days of frozen storage was doubled by HIUS induction. Furthermore, it was found that the improvement of EWP foamability was mainly due to the enhancement of surface hydrophobicity and the decrease of apparent viscosity, which increased the diffusion rate of protein to the interface and its adsorption amount at the interface. These results showed that HIUS was a simple, efficient and residue free way to improve the foam characteristics of frozen EWP, which has strong promotion and application value.

1. Introduction

Egg white is usually used as a key ingredient in different food systems (e.g. bakery foods, meat products, confectionary etc.) because of its outstanding functional properties (foaming, emulsifying, gelatinous), giving the product unique sensory, texture and taste [1, 2]. Owing to the fresh liquid egg white is rich in protein system and is easy to be microbial contamination in the process of separation from egg shell [3]. At present, pasteurization is usually used commercially to ensure the microbial safety of fresh egg white. However, the thermal sterilization process will inevitably lead to partial aggregation of proteins, which will affect the interface properties of egg white [4–6]. Therefore, freezing, the most common preservation technology, is also a common choice to extend the shelf life of egg white [7]. Nevertheless, for high protein systems such as egg white, due to surface denaturation and freeze concentration effect, protein conformation will be unfolded, and a large number of aggregates will be formed during long-term frozen storage, so as to reduce the interface properties of proteins [7, 8].

Therefore, it is necessary to find a simple and efficient way to improve the interface properties of frozen egg white protein (EWP). In fact, in order to enhance the foam properties of EWP as much as possible to meet the processing needs of complex food systems, physical methods have gained the most interest [9]. For example, high-intensity ultrasound (HIUS) treatment could enhance the surface hydrophobicity of ovalbumin (OVA) and reduce the surface potential, so as to improve the emulsifying activity and foaming ability of OVA [10]. Similarly, after HIUS treatment, the free sulfhydryl content and surface hydrophobicity of fresh EWP enhanced, thereby its foaming ability was increased by 4.9 times [11]. In particular, Chen et al. treated EWP in different cold storage periods by ultrasound, which could improve its foam ability from 29.75–99.13%, and pointed out that this was mainly due to the enhancement of protein surface hydrophobicity and structural flexibility [1]. Besides, ultrasound-irradiation combined pretreatment could increase the solubility of liquid EWP, reduce the particle size, and enhance the foam ability of EWP [12]. Also, HIUS treatment could improve the emulsifying, foaming and gel properties of egg yolk by regulating the physicochemical properties of egg yolk and partial dissociation of yolk granules [13]. All these works

show that HIUS treatment has outstanding efficiency in improving the foam properties of EWP and egg yolk.

The foaming properties of protein are usually characterized by two main parameters: foamability and foam stability. The foaming property is related to the gas phase volume level when the gas is introduced into the protein solution, and is estimated by measuring the increase of foam volume. The stability of foam is determined by measuring the liquid discharge rate over time or the volume reduction rate of foam caused by bubble coalescence [14]. Hence, enhancing the diffusion rate of protein to the interface during the whipping contribute to improve its foaming ability, which is not only related to the physicochemical properties of the protein, but also depends on the bulk viscosity [15]. The enhancement of surface hydrophobicity and the decrease of size of proteins are generally considered to play a positive role in their diffusion to the interface, while the increase of surface net potential and bulk viscosity is a negative effect [16]. For these considerations, like HIUS, many other different approaches have been proved to be effective in improving the foam characteristics of EWP, which are attributed to the regulation of interface absorption behavior [17, 18].

Consequently, in this work, HIUS was selected to treat EWP with different freezing times to achieve the improvement of foam properties. In detail, the foaming ability, average size, zeta potential, surface hydrophobicity, and structure of EWP with different freezing time (0, 3, 7, 14, 21 days) were analyzed after HIUS treatment. In addition, the solution apparent viscosity and air-water interface adsorption behavior of EWP before and after ultrasonic treatment were also evaluated. Thus, it provided insights into the improvement of the foam characteristics of frozen EWP by HIUS treatment.

2. Materials And Methods

2.1 Materials

Fresh eggs (laying time was within 24 hours) were purchased from Wanda Mao yonghui supermarket in Qixia District, Nanjing. 8-anilinonaphthalene-sulfonic acid (ANSA) were purchased from Aladdin Reagent Company (Shanghai, China). Other reagents were obtained from Sinopharm Chemical Reagent Co., Ltd. (Shanghai, China). The water used in the experiment was deionized water unless otherwise specified.

2.2 High intensity ultrasound (HIUS) treatment of egg white protein (EWP)

The EWP and yolk of fresh eggs were separated manually. The EWP was collected and treated with a high-speed disperser (XHF-DY, Ningbo Xinzhi Biotechnology Co., Ltd., China) at 2800 r/min for 5 minutes to mix evenly. Then, EWP (25 mL) was sub packed into a 50 mL centrifuge tube and stored at -20 ℃. Samples were taken at different intervals (3, 7, 14, 21 days) and placed at room temperature to fully thaw it. After that, a 20 kHz high-intensity ultrasonic instrument (JY98-□DN, Ningbo Xinzhi Biotechnology Co., Ltd., China) with an 18 mm titanium probe was used to treat EWP dispersions for 5 min (working for 3 s, intermittent for 5 s) at 60% amplitude. In order to control the temperature during HIUS processing, the

samples were immersed in an ice water bath. Then, its foamability and other physicochemical properties were measured. Fresh egg liquid and thawed EWP without HIUS treatment were used as control. Samples without ultrasonic treatment at different times of frozen storage (0, 3, 7, 14, 21 days) were marked as E0, E3, E7, E14, E21 respectively, while samples after HIUS treatment were marked as E0-U, E3-U, E7-U, E14-U, E21-U.

2.3 Determination of EWP foaming properties

The determination of foam properties of the samples described in section 2.2 according to the method reported in the literature with slight modification [10]. Briefly, EWP solution (10 mL, V_0) was put into a centrifuge tube (50 mL), and treat it with a high-speed disperser at 8000 r/min for 2 min at room temperature. Foaming ability (FA) was measured by comparing the foam volume at 2 min with the initial liquid volume of sample. Foaming stability (FS) was determined by comparing the foam volume at 30 min with the initial foam volume of sample.

$$\mathrm{FA}\ (\%) = \frac{V_1}{V_0} \times 100$$

1

$$\mathrm{FS}\ (\%) = \frac{V_2}{V_1} \times 100$$

2

2.4 Particle size and zeta potential determination

As described in section 2.2, the sample was diluted to 0.5% (w/v) by phosphate buffer solution (pH 9.0, 10 mM), and then its zeta potential, average particle size and polydispersity index were measured by using ZS Zetasizer Nano (Malvern Instrument Ltd., UK). The measurement results are automatically given by the software, and the measurement temperature was room temperature.

2.5 Solubility measurements

The sample solution treated in section 2.2 was centrifuged at 10000g for 10min. The protein content of the supernatant was determined by bicinchoninic acid assay [19]. Solubility was expressed as the percentage of protein in the supernatant in the whole EWP solution.

2.6 Determination of surface hydrophobicity

The surface hydrophobicity of the samples (as described in Section 2.2) were determined by 8-anilinonaphthalene-sulfonic acid (ANSA) fluorescent probe. Briefly, ANSA solution (50 μL, 2.4 mM) was added to the sample solutions with different protein concentrations (5 mL, 0, 0.1, 0.2, 0.4, 0.6, 0.8, 1 mg/mL) and mixed evenly, and then measured with a fluorescence spectrophotometer (F-4600, Hitachi, Japan). The excitation and emission wavelength ranges were set to 385 nm and 400–650 nm

respectively, and the slit width was 5 nm. As a result, the linear slope formed by the maximum fluorescence intensity of samples with different protein concentrations was taken as the surface hydrophobicity value (H_0).

2.7 Intrinsic fluorescence spectrum

EWP solution (0.2 mg/mL) was placed in a quartz cuvette with an optical path of 1cm, and then its intrinsic fluorescence spectrum was characterized by using a fluorescence spectrometer (F-4600, Hitachi, Japan). The excitation wavelength and emission wavelength range were 285 nm and 300–460 nm respectively, and the slit width was 5 nm.

2.8 Determination of apparent viscosity

The apparent viscosity of EWP solution without dilution was measured by rotating rheometer (MCR302, Anton paar, Austria). The gap value between the conical plate (CP50-1) and the flat bottom was 60 μm. The shear rate range was 1–20 s^{-1}, and the temperature was set at 25 ℃. Results are presented as viscosity against shear rate and analyzed using the time-independent Cross model, as shown in Eq. (3) [20].

$$\eta = \eta_\infty + \frac{\eta_0 - \eta_\infty}{1 + \left(k\dot{\gamma}\right)^m}$$

3

Where η_∞ is the infinite viscosity at high shear rate, η_0 is the at zero shear limiting viscosity at low shear rate, k is a constant related with the rupture of the physical linkages, m is the power index, and $\dot{\gamma}$is shear rate (1/s).

2.9 Measurement of interface surface pressure

The time-dependent surface pressure (π) of EWP absorbed layer at the air-water was monitored by using automated drop tensiometer (OSA 60, Ningbo NB Scientific Instrument Co., Ltd, China) at 25°C as descripted in previous work [21]. EWP solution was placed in cuvette, and a bubble (10 μL) was formed by a syringe with a U-shaped needle. The instrument automatically calculates the interfacial tension by analyzing the drop shape, and then the surface pressure can be calculated by Eq. (4):

$\pi = \gamma_0 - \gamma$ (4)

In the equation, γ_0 (72.4 mN/m) and γ are the interfacial tension for air-deionized water and the air-sample solution, respectively. Additionally, a modified Ward and Tordai Eq. (4) was used to describe the change in surface pressure (π) as a function of adsorption time (t). Thus, for the system which adsorption process is controlled by protein diffusion, the slope of π versus $t^{1/2}$ curve can be used as the diffusion rate of protein to the interface.

$\pi = 2C_0K_BT(Dt/3.14)^{1/2}$ (5)

Where C_0 is the protein concentration in the bulk phase, K_B is Boltzmann constant, T is the absolute temperature, D is the diffusion constant, and t is the absorption time.

2.10 The amount of protein adsorbed at the interface

The measurement of the protein content in the foam was carried out according to the methods reported in the literature with slight modification [21]. In brief, the foam prepared as described in 2.3 was collected and lyophilized, and the protein concentration in the foam was determined using bicinchoninic acid. The amount of protein adsorption as a percentage of the protein content of the foam was accounted initial protein content.

2.11 Statistical analysis

All measurements were performed in triplicate unless otherwise stated. One-way analysis of variance (ANOVA) with a 95% confidence interval was used to assess the significance of the results obtained. Statistical analysis was carried out using SPSS 19.0

3. Results And Discussion

3.1 Foaming ability and foam stability

HIUS treatment can significantly enhance the foaming ability of EWP, which has been found in previous reports. For example, Sheng et al. Found that the foaming ability of fresh EWP increased by 4.9 times after sonication with 360 W (20 kHz) for 10 min [11]. However, Arzeni et al. found that after EWP was sonicated (frequency: 20 kHz; amplitude: 20%) for 20 minutes, the foam overrun value decreased from 205–127% [9]. This diversity should be attributed to the difference of ultrasonic processing parameters and protein sources. In present work, the foaming ability of fresh EWP increased by 36% after HIUS treatment (Fig. 1A). On the contrary, freezing led to the continuous decline of the foaming capacity of EWP from 110% to less than 80% (day 21). It should be pointed out that freeze-thaw cycle treatment could significantly increase the foamability and foaming stability of fresh EWP, which was mainly due to the repeated effect of ice crystals on protein conformation [22].

It is worth noting that the foaming ability of EWP with different frozen storage time after HIUS treatment is increased by 40%-60% compared with that of protein without sonication (Fig. 1A). Especially for EWP stored for 21 days, its foaming capacity was more than doubled after HIUS treatment. A similar improvement was also observed in the report on the foaming ability of EWP treated with ultrasound at different cold times [1]. On the other hand, there was almost no significant difference in foam stability among all samples (Fig. 1B). These results show that short-term (5 min) ultrasonic treatment has a prominent effect on improving the foam characteristics of frozen EWP. In fact, we also tried a longer

ultrasonic treatment time (10 and 15min), because compared with 5min sonication, the foaming ability of EWP was not significantly improved ($p > 0.05$), so the results were not shown.

3.2 Solubility and average size of EWP

The solubility of fresh EWP is about 57%, while that of sonicated EWP is increased to 73% (Fig. 2A). Sheng et al. observed that HIUS treatment could increase the solubility of fresh EWP from less than 60–90%, and this improvement did not depend on ultrasonic power [11]. However, Yu et al. found that the solubility of EWP decreased significantly after ultrasonic treatment [12]. These discrepancies should be related to the various experimental conditions. It is worth noting that the solubility of EWP continues to decline to about 30% with the extension of frozen storage time (Fig. 2A). This may be due to the enhanced freezing induced protein aggregation [7], which was easier to be separated into the precipitation in the process of solubility determination, thus showing a low solubility. After sonication, the solubility of all frozen samples increased significantly to about 70%. In addition to EWP, the same phenomenon was also observed in the reports of using HIUS treatment to improve the interface and physicochemical properties of soybean protein and whey protein isolate [23, 24].

From the average size shown in Fig. 2B, it can be found that the average diameter of fresh EWP increases from about 225 nm to 400 nm after ultrasonic treatment. Conversely, the poly diffusivity index (PDI) decreased significantly to 0.55, suggesting that the size distribution of protein aggregates induced by ultrasound was more concentrated. This result is consistent with past findings [1, 9, 10]. The increased solubility of EWP after ultrasonic treatment indicates that these particles should be soluble aggregates [12]. Similarly, the size of EWP with different freezing time increased significantly after HIUS treatment. Nevertheless, compared with fresh samples (232 nm), the average size of frozen EWP (150–225 nm) showed a significant reduction. In addition, the size of aggregates increased monotonously depending on the extension of freezing time, while the PDI value (0.5–0.6) did not change significantly. This phenomenon should be due to the destruction of ovomucoid and ovomucin in EWP by ice crystals due to short-term freezing (3 days), resulting in a significant reduction in size. With the increase of freezing time, the extrusion of ice crystals leads to protein aggregation and shows an increase in size [8, 22].

3.3 Apparent viscosity

The viscosity of protein solution will affect the adsorption rate of protein molecules to the air-water interface, and then impact the foam characteristics of protein. Obviously, fresh EWP shows a high constant viscosity (about 0.5 Pa.s) in the lower shear rate range (< 6 1/s), and a shear thinning non-Newtonian fluid behavior in the higher shear rate range (Fig. 3A). This phenomenon can be explained by the fact that ovomucoid and ovomucin contained in fresh EWP cause a large number of protein molecules to tangle together. The disruption and formation of these entanglements is balanced at low shear rates, ensuing higher constant viscosity (η_0) [25]. The mechanical energy produced by freezing and HIUS treatment destroyed the aggregation and structure of protein [22, 26], which significantly reduced the apparent viscosity of EWP. Therefore, the viscosity of samples at different freezing periods decreased

after further ultrasonic treatment (Fig. 3B). The same phenomenon was also observed in the treatment of fresh EWP with different power ultrasound [11].

Furthermore, in order to quantitatively compare the effects of freezing and HIUS treatment on EWP fluid behavior, the cross model was used to fit the data of apparent viscosity versus shear rate. The fitting parameter results are shown in Table 1, and the regression coefficient (R^2) shows that the model has a good fitting. For the samples without sonication, both infinite viscosity (η_∞) at high shear rate and zero shear limiting viscosity (η_0) at low shear rate showed a gradual decrease depending on the extension of freezing time. Similarly, the η_∞ and η_0 of the samples treated by HIUS were lower than that before ultrasonic treatment. On the other hand, compared with fresh EWP, the decrease of m value indicated that the strength of shear-thinning behavior was less obvious for all treated samples. In addition, the increase of *k* parameter implies that shear rate at which transition from Newtonian to shear-thinning behavior occurs shifts to lower values with the extension of freezing time. Also, HIUS treatment induced a remarkable increase in the *k* value of EWP in fresh and frozen samples for 3 days, but had no significant effect on frozen samples for 7 and 14 days. In particular, it is worth noting that the k value of EWP frozen for 21 days after acoustic energy treatment shows a sharp decrease, indicating that the increase of shear-thinning behavior rate. This result can also be obtained by comparing the fitting curve profile of samples frozen for 21 days before and after HIUS treatment (Fig. 3). This result may be related to the enhanced protein aggregation (size increase, Fig. 2B) caused by ultrasonic mechanical effect. These effects of freezing and subsequent HIUS treatment on EWP fluid behavior should be closely related to the diffusion rate of protein during whipping, especially the reduction of viscosity.

Table 1
Parameters of the Cross' model for the samples investaged.

	η_0(Pa.s)	η_∞(Pa.s)	$k(s^{-1})$	m	R^2
E0	0.506 ± 0.015	0.255 ± 0.023	0.103 ± 0.007	4.925 ± 1.610	0.926
E3	0.094 ± 0.003	0.014 ± 0.003	0.170 ± 0.007	1.956 ± 0.195	0.994
E7	0.084 ± 0.002	0.011 ± 0.001	0.267 ± 0.008	2.633 ± 0.170	0.996
E14	0.045 ± 0.001	0.009 ± 0.004	0.254 ± 0.007	1.985 ± 0.117	0.998
E21	0.043 ± 0.003	0.006 ± 0.002	0.631 ± 0.063	2.607 ± 0.298	0.994
E0-U	0.292 ± 0.016	0.012 ± 0.001	0.253 ± 0.028	1.322 ± 0.246	0.989
E3-U	0.092 ± 0.002	0.004 ± 0.001	0.235 ± 0.006	2.000 ± 0.116	0.999
E7-U	0.064 ± 0.003	0.002 ± 0.001	0.219 ± 0.014	1.647 ± 0.219	0.991
E14-U	0.014 ± 0.001	0.003 ± 0.001	0.206 ± 0.005	2.893 ± 0.174	0.996
E21-U	0.007 ± 0.001	0.003 ± 0.001	0.305 ± 0.024	1.932 ± 0.255	0.986

3.4 Zeta potential, surface hydrophobicity and intrinsic fluorescence

The surface potential of protein can reflect the changes of its conformational, and indicating the exposure of charged groups in the side chain of protein molecules. It can be seen from Fig. 4 that compared with fresh EWP, the zeta potential of most other samples changes slightly ($P > 0.05$), regardless frozen or ultrasonic treatment. This phenomenon is consistent with the performance of EWP in the long-term cold storage [1]. In addition, the absolute potential of EWP increased after 21 days of freezing, while HIUS treatment had no effect. This implied that freezing was the main factor inducing protein conformational transition, and the effect of HIUS was relatively weak.

Furthermore, the surface hydrophobicity (H_0) of fresh and frozen EWP for 21 days before and after ultrasonic treatment was characterized (Fig. 5A). It could be found that HIUS treatment has no significant impact on the surface hydrophobicity of fresh EWP. However, after 21 days of freezing, the H_0 value of egg white increased remarkably, and sonication further induced its enhancement. This result agreed with the findings of freeze-thaw cycle treatment[22]. For frozen EWP, the increase of surface hydrophobicity after ultrasonic treatment should be attributed to the cavitation, which leaded to protein aggregates to expose more hydrophobic micro regions. Moreover, intrinic fluorescence spectra were used to further confirm these results (Fig. 5B). As expected, ultrasonic treatment has little effect on the emission fluorescence curve of fresh EWP. This was different from most previous reports on EWP treatment with high-intensity ultrasound [1, 13, 27]. It was inferred that this discrepancy mainly derived from the diversification of ultrasonic treatment conditions. Also, a strong fluorescence emission peak can be observed at 335 nm for all samples after excitation at 280 nm. However, freezing and subsequent HIUS treatment resulted in a significant decrease in the fluorescence intensity of EWP compared with fresh samples. This phenomenon is similar to the result of ultrasonic treatment of OVA [10]. Since tyrosine and tryptophan residues can be excited simultaneously at 280 nm [28], the reduction of fluorescence intensity means that the chromophores of EWP become exposed to solvent and the transformation of tertiary conformation due to HIUS treatment. Besides, owing to the indole group of tryptophan is more hydrophobic than the phenol group of tyrosine and the enhanced results of surface hydrophobicity, it is speculated that freezing and subsequent ultrasonic treatment mainly induce the exposure of more tryptophan residues.

3.5 Interfacial adsorption behavior

Indeed, the improvement of foaming ability of frozen EWP after ultrasonic treatment was mainly due to the changes of the above physicochemical properties, which has an impact on the air-water interface adsorption behavior of protein. The plots of surface pressure (π) versus time ($t^{1/2}$) exhibited the same profile, and π value showed a continuous increase due to the absorption of proteins (Fig. 6A). It can be found that within 400s of the initial stage of adsorption, the π values of all samples show a linear rapid increase trend, and then gradually reach a platform region. The slope of the linear region could be fitted

by a modified ward and Tordai equation (the fitting curves are the red dotted lines in Fig. 6A), and was used as the diffusion rate of protein to the air-water interface (K_{diff}, Fig. 6B). Compared with fresh EWP, ultrasonic treatment alone led to a significant increase in the diffusion rate. Nevertheless, long-term freezing and subsequent cavitation can not remarkably affect its K_{diff} compared with sonicated fresh EWP (Fig. 6C). Additionally, the surface pressure of the selected samples at the beginning (π0) and end point (π10800) of adsorption has been significantly increased after ultrasonic treatment compared with fresh samples (Fig. 6C). On the other hand, after ultrasonic and freezing treatment, the amount of protein adsorption at the air-water interface are significantly higher than fresh EWP (Fig. 6D). The difference of these interface behavior parameters should be attributed to the discrepancy of physicochemical properties of continuous phase and protein.

Firstly, the π0 value of protein is weakly correlated with the properties of bulk phase (such as viscosity), which is mainly determined by the physicochemical properties of aggregates [29, 30]. Generally, the increase of surface hydrophobicity and the decrease of average size of proteins are conducive to driving their shifting to the interface, while the increase of zeta potential will hinder the diffusion due to the enhancement of intermolecular repulsion force [6, 31–34]. Therefore, the increase of π0 of EWP (E0-U and E21-U) after HIUS treatment was mainly contributed by the surface hydrophobicity. Secondly, with the continuous adsorption, the diffusion of protein to the interface depends on its own physicochemical properties and bulk viscosity. Obviously, the decrease of viscosity and the enhancement of surface hydrophobicity dominated the migration of proteins to the interface, resulting in a significant increase in the diffusion rate of samples (E0-U, E21 and E21-U), although the average size and zeta potential were increased by ultrasound and freezing treatment. Finally, the increase of surface pressure (π10800) and interfacial adsorption capacity of the ultrasonic treated samples at the end of adsorption should also be mainly attributed to the enhancement of surface hydrophobicity. Therefore, although freezing and ultrasonic treatment leaded to the increase of the average size and surface potential strength of EWP, which was not conducive to the diffusion of protein to the interface. Instead, the decrease of bulk phase viscosity and the enhancement of surface hydrophobicity play a more important role, thereby EWP showed stronger foamability.

4. Conclusions

In summary, the foaming ability of fresh egg white protein (EWP) after 21 days of frozen storage decreased by about 30%. The foaming ability of EWP with different freezing period after HIUS treatment could be significantly improved, especially the EWP after 21 days of frozen storage could be doubled. Through the investigation of protein structure and physicochemical properties, it was found that this improvement was mainly due to the enhancement of protein surface hydrophobicity and the decrease of egg white viscosity. Although ultrasonic cavitation and freezing leaded to the increase of protein aggregate size and potential, it was not conducive to its diffusion to the interface. These findings indicated that high-intensity ultrasound was a method that could effectively improve the foaming characteristics of frozen EWP, and has outstanding application value.

Declarations

Conflict of Interest: The authors declare that they have no conflict of interest.

Acknowledgments

The authors thank the financial support from the Key Laboratory of Food Nutrition and Functional Food of Hainan Province (No. KF202005), Natural Science Foundation of China (NSFC, No. 31860454) and A Project Funded by the Priority Academic Program Development of Jiangsu Higher Education Institutions （PAPD）.

Author Contribution

Ya Li and Ling Yu performed the experiments, prepared the figures and tables, analyzed the data regarding and wrote the manuscript. Wenfei Xiong designed the experimental protocol. Lifeng Wang and Wenfei Xiong contributed to data interpretation and editing the manuscript. All authors read and approved the final manuscript.

References

1. Y. Chen, L. Sheng, M. Gouda, M. Ma, LWT-Food Sci. Technol. **113**, 108303 (2019)
2. J. O'Sullivan, B. Murray, C. Flynn, I. Norton, Food Hydrocolloid. **53**, 141–154 (2016)
3. J. Zhu, D. Zhang, X. Zhou, Y. Cui, S. Jiao, X. Shi, Food Control **123**, 107035 (2021)
4. C.-Y. Ma, V.R. Harwalkar, L.M. Poste, M.R. Sahasrabudhe, Food Res. Int. **26**(4), 247–254 (1993)
5. V. Lechevalier, C. Guérin-Dubiard, M. Anton, V. Beaumal, E.D. Briand, A. Gillard, Y. Le Gouar, N. Musikaphun, G. Tanguy, M. Pasco, D. Dupont, F. Nau, J. Food Eng. **195**, 137–149 (2017)
6. V. Plancken, I.A. Van Loey, M.E. Hendrickx, J. Food Eng. **78**(4), 1410–1426 (2007)
7. B. Fang, K. Isobe, A. Handa, K. Nakagawa, J. Food Eng. **296**, 110452 (2021)
8. M.C. Erickson, Y.C. Hung, *Quality in frozen food* (Springer Science & Business Media, 2012), pp. 131–159
9. C. Arzeni, O.E. Pérez, A.M.R. Pilosof, Food Hydrocolloid. **29**(2), 308–316 (2012)
10. W. Xiong, Y. Wang, C. Zhang, J. Wan, B.R. Shah, Y. Pei, B. Zhou, J. Li, B. Li, Ultrason. Sonochem **31**, 302–309 (2016)
11. L. Sheng, Y. Wang, J. Chen, J.Z.Q. Wang, M. Ma, Food Res. Int. **108**, 604–610 (2018)
12. Y. Yu, H. Zhang, J. Zhu, J. Liu, T. Zhang, J. Food Sci. **85**(12), 4312–4318 (2020)
13. Y. Xie, J. Wang, Y. Wang, D. Wu, D. Liang, H. Ye, Z. Cai, M. Ma, F. Geng, Ultrason. Sonochem **60**, 104767 (2020)
14. C. I.Nicorescu, E. Vial, V. Talansier, C. Lechevalier, D. Loisel, A. Della Valle, G. Riaublanc, Djelveh, J. Legrand Food Hydrocolloid **25**(4), 797–808 (2011)

15. F. Alavi, Z. Emam-Djomeh, M. Mohammadian, M. Salami, A.A. Moosavi-Movahedi, Food Hydrocolloid **101**, 105554 (2020)
16. M.S. Sadahira, M.I. Rodrigues, M. Akhtar, B.S. Murray, F.M. Netto, Food Hydrocolloid **58**, 1–10 (2016)
17. L. Ding, M. Xia, Q. Zeng, Q. Zhao, Z. Cai, Z. Zhu, LWT-Food Sci. Technol. **153**, 112505 (2022)
18. X. Li, Y. Yang, B.S. Murray, A. Sarkar, J. Food Eng. **275**, 109860 (2020)
19. W. Xiong, Q. Deng, J. Li, B. Li, Q. Zhong, Food Hydrocolloid **98**, 105282 (2020)
20. D.Reinoso, M.J.Martín-Alfonso, P.F.Luckham, F.J.Martínez-Boz, Carbohydr. Polym. **203**, 103–109 (2019)
21. W. Xiong, J. Li, B. Li, L. Wang, Food Hydrocolloid. **97**, 105210 (2019)
22. X. Duan, J. Li, Q. Zhang, T. Zhao, M. Li, X. Xu, X. Liu, Food Chem. **228**, 243–248 (2017)
23. M. Zhou, J. Liu, Y. Zhou, X. Huang, F. Liu, S. Pan, H. Hu, Innov. Food Sci. Emerg. **34**, 205–213 (2016)
24. R. Shi, Y. Liu, J. Hu, H. Gao, A. Qayum, A. Bilawal, G. Munkh-Amgalan, Z. Jiang, J. Hou, Innov. Food Sci. Emerg. **65**, 102450 (2020)
25. N. Repin, S.W. Cui, H.D. Goff, Food Hydrocolloid **76**, 216–225 (2018)
26. M. Uygun-Sarıbay, E. Ergun, Y. Kalaycı, T. Köseoğlu, Int. J. Food Prop. **20**, 1195–1203 (2017)
27. Y. Chen, M. Ma, Food Hydrocolloid **102**, 105568 (2020)
28. V. Lechevalier, T. Croguennec, S. Pezennec, C. Guérin-Dubiard, M. Pasco, F. Nau, J. Agric. Food Chem. **51**(21), 6354–6361 (2003)
29. T. Croguennec, A. Renault, S. Beaufils, J.J. Dubois, S. Pezenne, J. Colloid Interface Sci. **315**(2), ,627 (2007) – 36(2007).
30. C.Le Floch-Fouéré, S. Beaufils, V. Lechevalier, F. Nau, M.P.ézolet,A. Renault, S.Pezennec, Food Hydrocolloid. **24**(4), ,275–284 (2010)
31. X. Yang, T.K. Berry, E.A. Foegeding, J. Food Sci. **74**(5), E259–E268 (2009)
32. T.K. Berry, X. Yang, E.A. Foegeding, J. Food Sci. **74**(5), E269–E277 (2009)
33. Y. Liang, H.G. Kristinsson, Food Res. Int. **40**(6), 668–678 (2007)
34. P.A. Wierenga, M.B.J. Meinders, M.R. Egmond, F.A.G.J. Voragen, H. H. J. de Jongh, Langmuir **19**(21), 8964–8970 (2003)

Figures

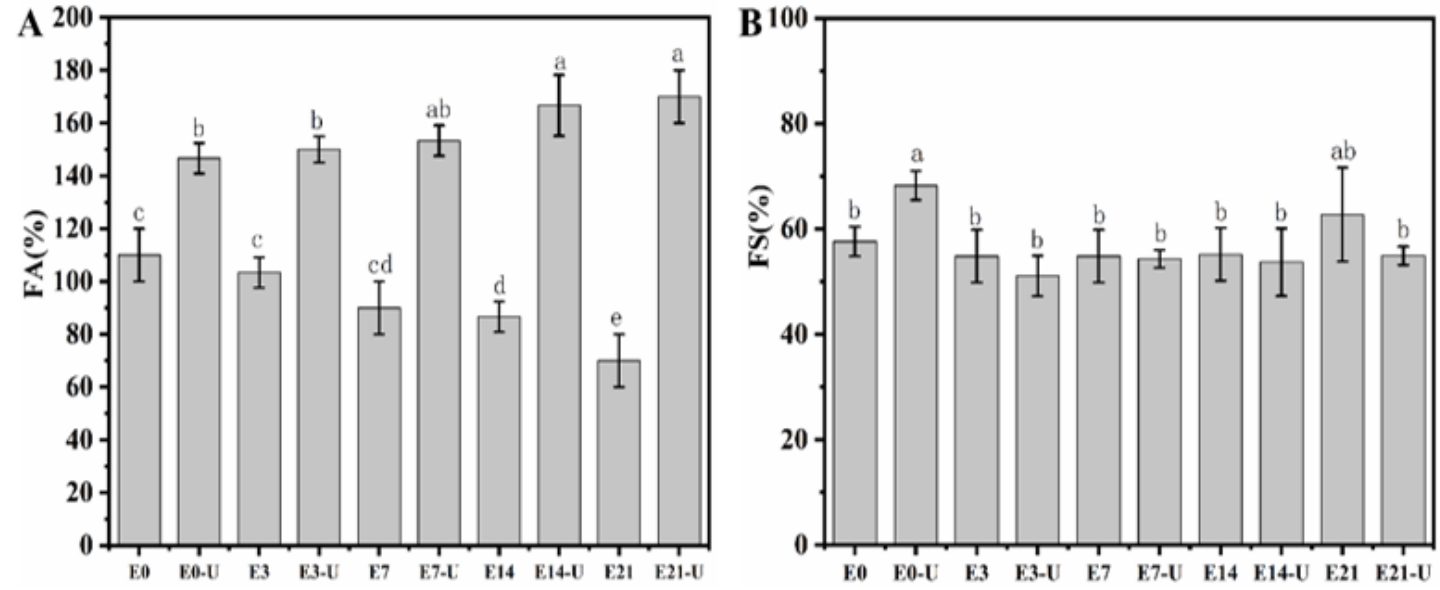

Figure 1

Foaming ability (A) and foaming stability (B) of frozen EWP before and after HIUS treatment. Each column shows the mean ± SD (n = 3), means in same column with different letters are significantly different ($P < 0.05$).

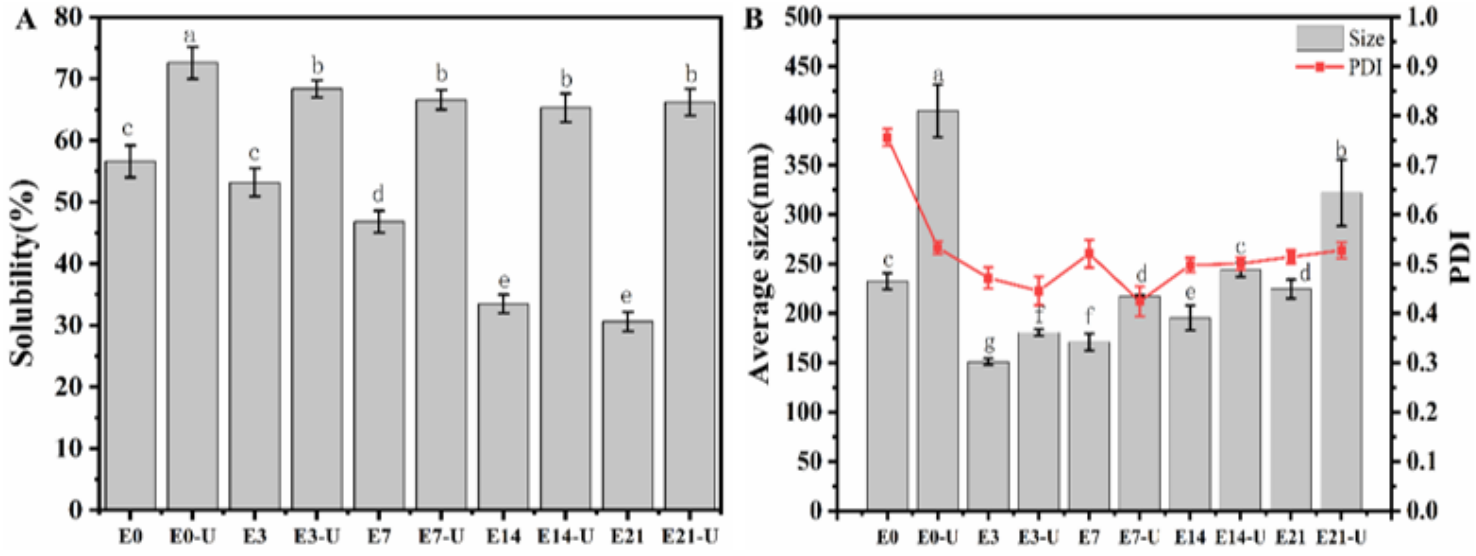

Figure 2

Solubility (A), average size and poly diffusivity index (PDI) (B) of frozen EWP before and after HIUS treatment. Each column shows the mean ± SD (n = 3), means in same column with different letters are significantly different ($P < 0.05$).

Figure 3

Apparent shear viscosity of frozen EWP before (A) and after (B) HIUS treatment. The dotted line is the fitting result of cross model

Figure 4

Zeta potential of frozen EWP before and after HIUS treatment. Each column shows the mean ± SD (n = 3), means in same column with different letters are significantly different ($P < 0.05$).

Figure 5

Surface hydrophobicity (A) and intrinsic fluorescence spectrum (B) of frozen EWP before and after HIUS treatment. Each column shows the mean ± SD (n = 3), means in same column with different letters are significantly different ($P < 0.05$).

Figure 6

(A) Square root of time ($t^{1/2}$) dependence of surface pressure (π) for frozen and sonicated EWP adsorbed layers at the air-water interface. K_{diff} represent diffusion rate. (B) K_{diff} of pretreated frozen and sonicated EWP. (C) Surface pressure after 3 h of adsorption of frozen and sonicated EWP. (D) Effect of ionic strength on the amount of protein adsorbed at the air-water interface. Each column shows the mean ± SD (n = 3), means in same column with different letters are significantly different ($P < 0.05$).